Int. J. Electrochem. Sci., 11 **(2016)** 5829 – 5837, doi: 10.20964/2016.07.60

International Journal of
ELECTROCHEMICAL
SCIENCE
www.electrochemsci.org

Improving Electrochemical Performance of Fe doped $Li_{1.2}Ni_{0.13}Co_{0.13}Mn_{0.54}O_2$ Cathode Material for Lithium-Ion Battery

Xinghua Liang[*], *Hanjie Wu*

Guangxi Key Laboratory of Automobile Components and Vehicle Technology, Guangxi University of Science and Technology, Liuzhou 545600, China
[*]E-mail: liangxinghua888@163.com

Received: 19 April 2016 / *Accepted:* 22 May 2016 / *Published:* 4 June 2016

$Li_{1.2}Ni_{0.13}Co_{0.13}Mn_{0.54}O_2$ cathode material was prepared via a high temperature solid-state method. Using X-ray diffraction, scanning election microscopy, electron diffraction spectroscopy, infrared absorption spectrum, electrochemical impedance spectroscopy (EIS), and galvanostatic charge-discharge measurements. The $Li_{1.2}Ni_{0.13}Co_{0.13}Mn_{0.54}O_2$ electrode appears a high reversible discharge capacity of 300 mAhg-1 at 0.1C-rate with a high capacity retention rate of 90.9% after 50 cycles within a potential range of 2.0-4.8 V at room temperature. The Fe-doped cathode materials indicate a better improvement in cycling performance and rate character, which EIS datas indicated a number of variation in surface film resistance (Rs) and lithium intercalation/de-intercalation resistance (Rct) as a function of applied voltage. The datas indicate well-crystallized surface of the particles and stability of layered structure of $Li_{1.2}Ni_{0.13}Co_{0.13}Fe_{0.02}Mn_{0.52}O_2$ electrode with amorphous surface area and spinel nanodonmains distribution for $Li_{1.2}Ni_{0.13}Co_{0.13}Mn_{0.54}O_2$ electrode at cycling, which explain the excellent electrochemical performance of Fe doped $Li_{1.2}Ni_{0.13}Co_{0.13}Mn_{0.54}O_2$ cathode material.

Keywords: Cathode material; Fe doping; electrochemical performance

1. INTRODUCTION

In order to achieve the demand better power densities and better energy, which is very significant to improve the cathode has a large specific ability of next-generation lithium-ion batteries [1-8]. In a recent period of time, layered lithium-rich materials $xLi_2MnO_3 \cdot (1\text{-}x)LiMO_2$(M=Co, Ni, $Mn_{1/2}Ni_{1/2}$, $Mn_{1/3}Ni_{1/3}Co_{1/3}$, etc) are being intensively studied for better cathode materials owning to their high capacity (>200mAh·g^{-1}) and low cost in comparison with $LiCoO_2$ and $LiFePO_4$ [9-10]. Among $Li_2MnO_3 \cdot LiMnO_2$ solid-state, Ni and Co-substituted Li_2MnO_3 cathode material, especially $Li_{1.2}Ni_{0.13}Co_{0.13}Mn_{0.54}O_2$, exhibits excellent electrochemical performance [8].

Low cycling stability makes the Mn-based Li-rich promising electrical energy storage system for many applications [11-17]. Present preparation methods (among the mixed lithium cobalt, nickel salt, salt, manganese salt [18-21]) as a result of nano-sized in order to poverty rate character. The poor electron transfer (i.e., poor ionic conductivity, which in turn affects Li_2MnO_3 component) while Li_2MnO_3 suffers from structural stability during electrochemical cycling(lithium diffusion in Li_2MnO_3 component in the activation of high current rates) [19].

Fe doping content is of great important to the structure and electrochemical properties of $Li_2MnO_3{\cdot}LiMnO_2$ solid-state. Li_2MnO_3-based materials with high Fe content above 10% show the obvious coexistence of layered phase (hexagonal crystal system) and cubic rock-salt phase(cubic crystal system) [22-24].

2. EXPERIMENTAL

2.1. Synthesis and characterization

Pristine oxide $Li_{1.2}Ni_{0.13}Co_{0.13}Mn_{0.54}O_2$ and Fe-doped $Li_{1.2}Ni_{0.13}Co_{0.13}Fe_xMn_{0.54-x}O_2$ (x=0, 0.01, 0.02, 0.03) denoted as LNCFM0, LNCFM1, LNCFM2 and LNCFM3 were synthesized by a high temperature solid-state method. $LiOH{\cdot}H_2O$ (AR 99.99% pure), cobalt acetate $Co(CH_3COO)_2{\cdot}4H_2O$ (AR 99.5% pure), nickel acetate $Ni(CH_3COO)_2{\cdot}4H_2O$ (AR 98.0% pure), magnesium acetate ferrum oxidation Fe_2O_3 (AR 98.5% pure) and $Mn(CH_3COO)_2{\cdot}4H_2O$ (AR 99.99% pure) were mixed within ball mill. The mixture was burned to get pure LNCFM0, LNCFM1, LNCFM2 and LNCFM3 powder in 25℃ temperature condition. Rietveld refinement of XRD data (2θ range from 10°-90°) was performed using Cu Kα radiation. The particle morphological assessment was examined using EVO-18 scanning electron microscopy. The microstructure and EDS were observed by SEM. By the means of the tabletting method, through infrared absorption spectrometer BIO-RED FTS300 detecting the crystallization properties and crystal structure of the samples.

2.2. Electrochemical measurements

The electrochemical measurements of samples were via CR2016 cells. The Galvanostatic charge and discharge tests were using Wuhan Hengdian Gaoce Electric (CT3008W-5V5mA-S4, China) from 2.0 to 4.8 V (vs. Li_0/Li^+) with charge and discharge rate of 0.1C, 0.2C, 0.3C, 0.5C, 0.8Cand 1C (1C=250 $mA{\cdot}g^{-1}$). Electrochemical impedance spectroscopy measurements were showed over an electrochemical workstation (CHInstrument 660E, China). The EIS measurements were showed on a frequency range from 10 mHz to 100 kHz.

3. RESULTS AND DISCUSSION

3.1. Crystal structures and particle morphology analysis

The X-ray diffraction (XRD) was studied the effect of Fe replaced crystal structure. As the typical hierarchical structure, visible impurity of all the $Li_{1.2}Ni_{0.13}Co_{0.13}Fe_xMn_{0.54-x}O_2$ samples cannot

be manifested. Figure 1 shows XRD curves of LNCFM0, LNCFM1, LNCFM2 and LNCFM3, manifesting a typical α-$NaFeO_2$ hexagonal. Mainly reflects on the basis of all the samples can be indexed hexagonal R-3m unit cells, and the weak supper-lattice reflection. The weaker peaks around 2θ=21°-24° manifest the superlattice commanded $LiMn_6$ which possess in monoclinic Li_2MnO_3 stage and the space group symmetry of C2/m [25-27]. The results of XRD refinement based on R3-m $Li_{1.2}Ni_{0.13}Co_{0.13}Fe_xMn_{0.54-x}O_2$ materials using space group rietveld method listed in Table 1. "c" can be seen that the lattice parameters of doped materials than the original materials, show that iron doped increase Intel-slab distance. These peaks short-range Li-Mn cation order transition metal layer [28,29]. Low intensity and peak broadening originates from $LiMn_6$ cluster obstacles and superlattice layer stacking fault along the "c" axis system [30-32]. At the same time, since the ionic radius of Fe^{3+} (0.63Å) is similar of Li^+ (0.76Å), the size of the occupation of lee layer of iron is likely [33,34]. Data show that when doped with trace amounts of Fe (x = 0.02), there is almost no slight increase in the lattice parameter changes but a little of c - lattice parameters and observed that the increase of cell volume. Morphology of these materials is research by means of scanning electron microscope, as shown in Figure 2, show that the material is consist of small particles have no obvious aggregation. The formation of the uniformed particles (50-300 nm in diameter) can be attributed to the use of chelating agent (citric acid). Can see smaller LNCFM2 exhibition in their better electrochemical performance. Energy dispersive spectrum studies have investigated their elements. The characteristic peaks of iron, manganese, nickel, and can be observed at Figure 3, li mountain peaks, and cannot be observed because lower relative atomic mass. Can infer, iron exists in the sample. Comb EDS and XRD patterns, atomic percentage (%) the proportion of each sample are listed in Table 2. Can prove that successfully doped into the target materials of Fe. IR spectra of LNCAM samples showed in Fig. 4 By data analysis, the bands at 598.17 and 522.93 cm^{-1} resulted from anti-symmetric elastic oscillation of Mn (IV)-O and Mn (III)-O in LNCAM crystal (Mn (IV) O_6 and Mn (III) O_6 octahedron), the weak band at 893.19 and 1490.72 cm^{-1} resulted from anti-symmetric elastic oscillation of Li-O and Fe-O in the LNCFM (LiO_4 and Fe_2O_3 tetrahedron). Therefore, the above illustrate the Fe and LNCMO combines together.

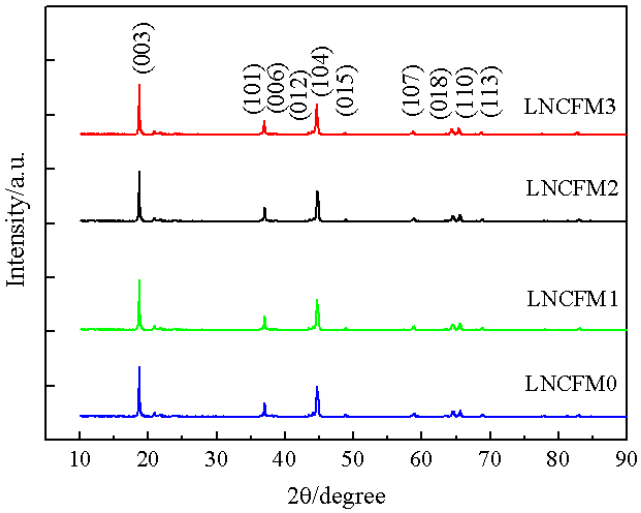

Figure 1. Powder XRD patterns of sample.

Table 1. Refinement agreements and lattice parameters of XRD data for LNCFM0, LNCFM1, LNCFM2 and LNCFM3.

Sample	a/Å	c/Å	c/a	Volume/Å3
LNCFM3	2.8551	14.475	5.0698	102.050
LNCFM2	2.8581	14.736	5.1559	102.461
LNCFM1	2.8517	14.318	5.0209	101.293
LNCFM0	2.8501	14.157	4.9672	100.078

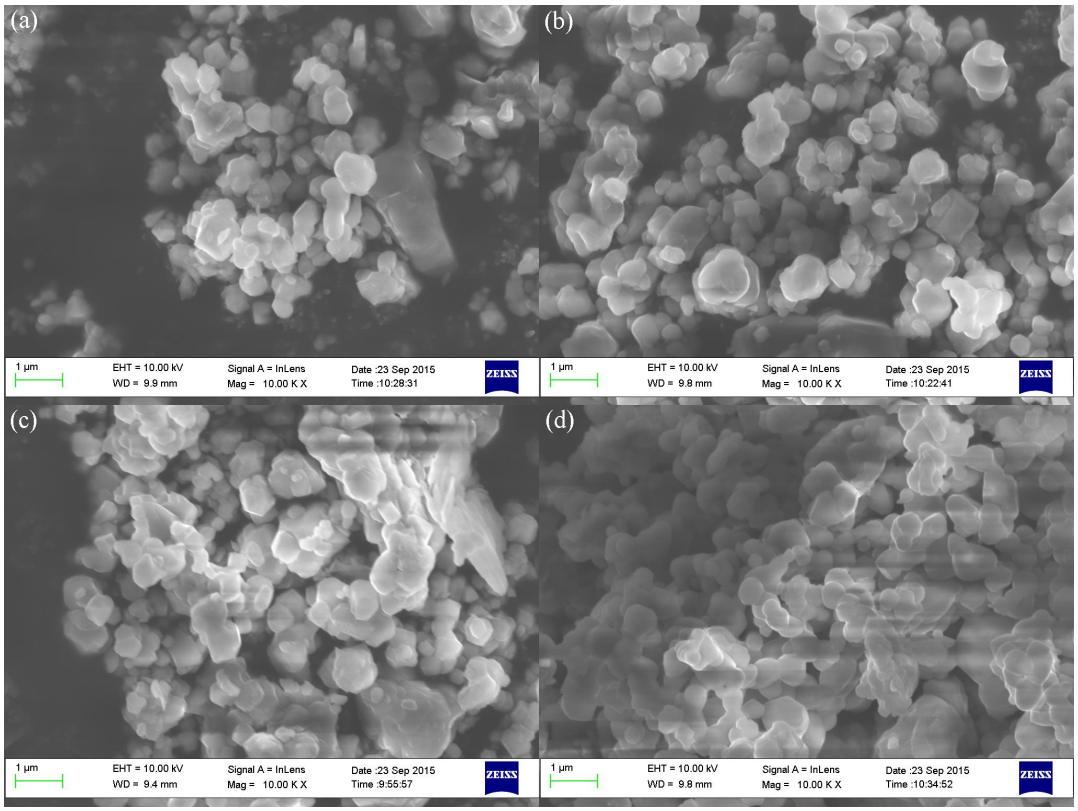

Figure 2. SEM pattern of LNCFM0, LNCFM1, LNCFM2 and LNCFM3.

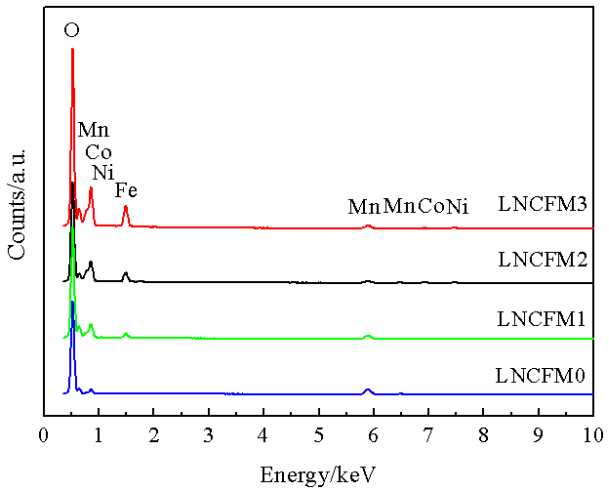

Figure 3. EDS spectrum of samples.

Table 2. Percentage (%) ratio of element O, Fe, Mn, Co and Ni in $Li_{1.2}Ni_{0.13}Co_{0.13}Fe_xMn_{0.54-x}O_2$ (x=0, 0.01, 0.02, 0.03).

Element	LNCFM0 (%)	LNCFM1 (%)	LNCFM2 (%)	LNCFM3 (%)
O	70.62	68.03	67.02	65.28
Fe	0	1.29	2.14	3.28
Mn	17.65	16.21	15.09	14.11
Co	5.17	6.39	7.21	8.68
Ni	6.56	8.08	8.54	8.65
Sum	100	100	100	100

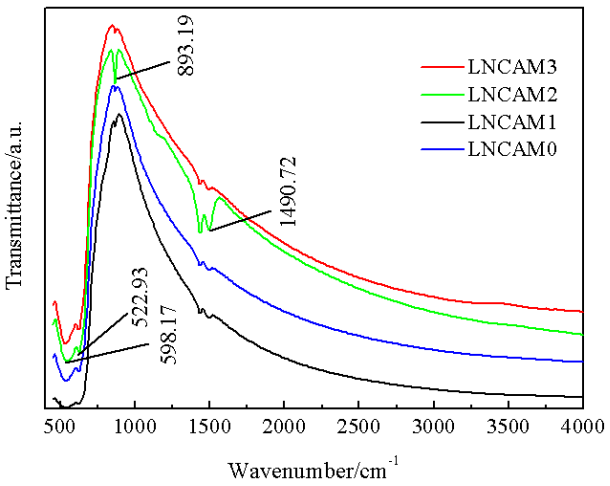

Figure 4. Infrared absorption spectrom of samples.

3.2 Galvanostatic charge-discharge characterisation

The charge and discharge curves of the as-prepared materials are shown in Fig. 5. The rate as a function of charge-discharge capacities for LNCFM0, LNCFM1, LNCFM2 and LNCFM3 between 0.1C (25 $mA \cdot g^{-1}$) to 2C (500 $mA \cdot g^{-1}$). $Li_{1.2}Ni_{0.13}Co_{0.13}Fe_xMn_{0.54-x}O_2$ could provide a better reversible capacity about 330 $mA \cdot g^{-1}$ at 0.1C. Original discharge capacity reduce significantly at higher current density, which discharge capacity at 1C is 113 $mA \cdot g^{-1}$, the level is only 40%. In comparision with the pristine material, the modified materials can show higher discharged capacities and rate performance due to $Li_{1.2}Ni_{0.13}Co_{0.13}Fe_{0.02}Mn_{0.52}O_2$ is 332.11 $mAh \cdot g^{-1}$, 308.86 $mAh \cdot g^{-1}$, 271.06 $mAh \cdot g^{-1}$ and 191.56 $mAh \cdot g^{-1}$, 113.92 $mAh \cdot g^{-1}$ at 0.1C, 0.2C, 0.5C, 1C and 2C after 50th cycle. Fig. 6. shows cycling performance of LNCFM0, LNCFM1, LNCFM2 and LNCFM3 at a current density of 25 $mA \cdot g^{-1}$ from 2.0-4.8, better cycling stability according to the modified samples show enhanced capacity retention are 97% after 50 cycles. This excellent electrochemical performance of $Li_{1.2}Ni_{0.13}Co_{0.13}Mn_{0.54}O_2$ cathode material is attributed to the Fe doping [35].

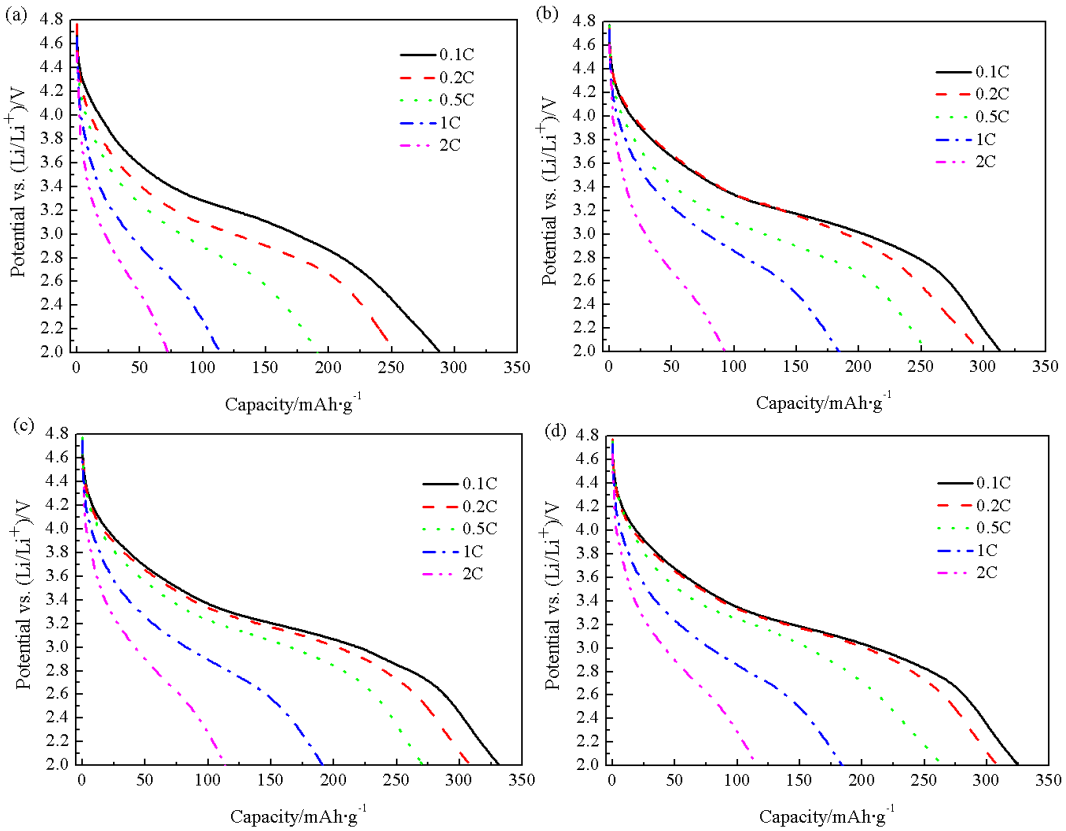

Figure 5. Discharge curves of $Li_{1.2}Ni_{0.13}Co_{0.13}Fe_xMn_{0.54-x}O_2$ as cathodes at various rates, (a) LNCFM0, (b) LNCFM1, (c) LNCFM2, (d) LNCFM3.

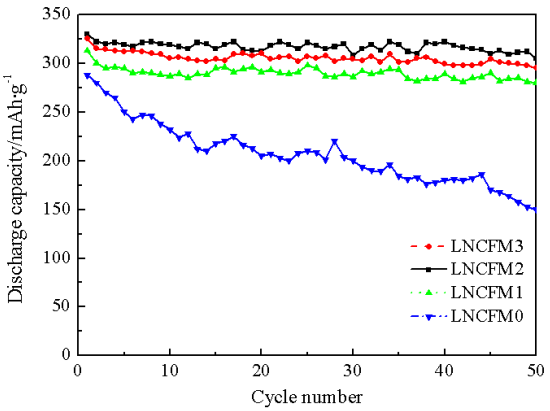

Figure 6. Cycling performance of LNCFM0, LNCFM1, LNCFM2 and LNCFM3.

3.3 Electrochemical impedance spectroscopic analysis

EIS is regarded as the ohmic polarization to know all kinds of situation occurred in electrodes/electrolyte interface. Comparing EIS spectroscopy of LNCFM0, LNCFM1, LNCFM2 and LNCFM3 electrode before EIS measurements and after 50 cycles at 0.25 $mA \cdot g^{-1}$ is shown in Fig. 7. Observing much smaller charge transfer resistance and semicircle in the high-frequency region in Fig. 7 (a). After 50 cycles, extra migration and electrochemical process of load transfer in the membrane surface during cycling is shown in Fig. 7 (b). The data after using proposed equivalent electrical circuit

is exhibited in Table 3 where Rs is lithium ion in the active material of the solid diffusion impedance. Before cycling, Rct value of LNCFM0 electrode is 828.3 Ω while LNCFM2 sample electrode shows lower Rct value of 168.4 Ω. After 50 cycles at 25 $mA \cdot g^{-1}$, Rct values of both samples greatly reduce, resulting in electrochemical activation. The Rct value of LNCFM2 electrode is 92.6 Ω in contrast to 217.1 Ω for LNCFM0 electrode. As mentioned above, LNCFM2 electrode has a higher diffusion coefficient to ride a bicycle, to reduce a randomized controlled trial values and improve the electrochemical performance.

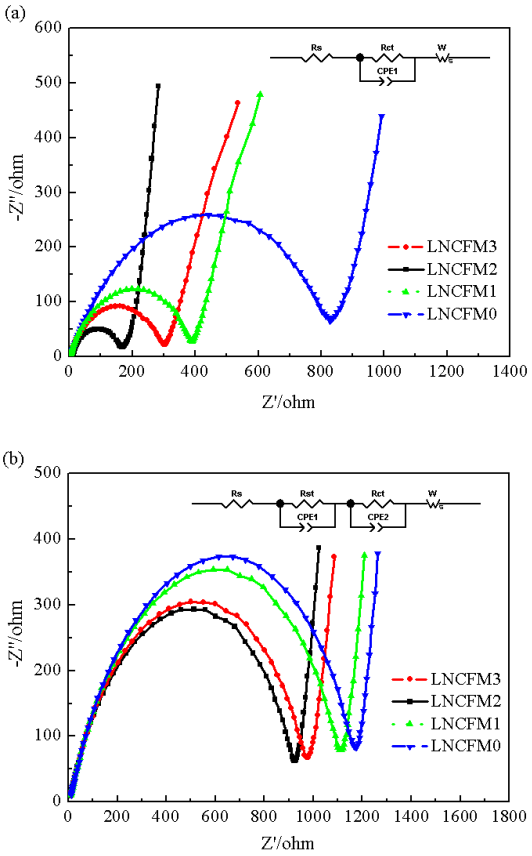

Figure 7. Discharge curves of $Li_{1.2}Ni_{0.13}Co_{0.13}Fe_xMn_{0.54-x}O_2$ as cathodes at various rates: (a) LNCFM0, (b) LNCFM1, (c) LNCFM2, (d) LNCFM3.

Table 3. The data after using proposed equivalent electrical circuit shown in the inset of Fig 7.

Samples	Before cycling		After 50 cycles	
	Rs	Rct	Rs	Rst+Rct
LNCAM3	5.606	301.4	9.981	97.4
LNCAM2	5.201	168.4	9.477	92.6
LNCAM1	5.973	390.9	10.640	111.2
LNCAM0	9.437	828.3	17.990	217.1

4. CONCLUSION

$Li_{1.2}Ni_{0.13}Co_{0.13}Mn_{0.54}O_2$ cathode material was prepared via a high temperature solid-state method. In comparision with the pristine material, the modified materials can show higher discharged capacities and rate performance due to $Li_{1.2}Ni_{0.13}Co_{0.13}Fe_{0.02}Mn_{0.52}O_2$ is 332.11 $mAh \cdot g^{-1}$, 308.86 $mAh \cdot g^{-1}$, 271.06 $mAh \cdot g^{-1}$ and 191.56 $mAh \cdot g^{-1}$, 113.92 $mAh \cdot g^{-1}$ at 0.1C, 0.2C, 0.5C, 1C and 2C after 50th cycle. LNCFM2 electrode has a higher diffusion coefficient to ride a bicycle, to reduce a randomized controlled trial values and improve the electrochemical performance. This excellent electrochemical performance of $Li_{1.2}Ni_{0.13}Co_{0.13}Mn_{0.54}O_2$ cathode material is attributed to the Fe doping.

ACKNOWLEDGEMENTS
This project was funded by the Project (No.15-A-03-01) of Guangxi Key Laboratory of Automobile Components and Vehicle Technology and the Innovation Project of Guangxi Graduate Education (YCSZ2015210). It was supported by the Innovation Project of Guangxi University of Science and Technology Graduate.

References

1. Z. Lu, D. D. Macneil and J. R. Dahn, E. *Solid-State Lett*, 34 (2001) 91.
2. L. Croguennec, J. Bains, J. Breger, C. Tessier and P. Biensan, *J. Power Sources*, 158 (2011) A665.
3. L. Z. Zhou, Q. J. Xu, M. S. Liu and X. Jin, *S. State Lonics*, 245 (2013) 135.
4. H. Liu, Y. Wang, L. Li, K. Wang, E. Hosono and H. Zhou, *J. Materials Chemistry*,19 (2009) 7889.
5. H. Liu, Y. Wang, K. Wang, E. Hosono and H. Zhou, *J. Materials Chemistry*,19 (2009) 2839.
6. D. C. Li, T. Muta, L. Q. Zhang, M. Yoshio and H. Noguchi, *J. Power Sources*, 132 (2004) 152.
7. D. C. Li, H. Noguchi and M. Yoshio, *Electrochimica Acta*, 50 (2004) 428.
8. A. C. Larson, R. B and V. Dreele, *L. Alamos Natl Lab*, 86 (1994) 748.
9. X. Jin, Q.Xu, H.Liu, X.Yuan and Y.Xia, Electrochimica Acta, 136 (2014) 19.
10. Z. Lu, J. R. Dahn, *J. Electrochem.Soc*, 49 (2002) 815.
11. C. J. Jafta, K. I. Ozoemena, M. K. Mathe and W. D. Roos, *Electrochimica Acta*, 85 (2012) 412.
12. Y. K. Sun, M. G. Kim, S. H. Kang and K. Amine, *J. Mater.Chem*, 13 (2003) 319.
13. C. W. Lee, Y. K. Sun, J. Prakash, *Electrochimica Acta*, 49 (2004) 4425.
14. Q. Liu, K. Du, H. Guo, Z. Peng, Y. Cao and G. Hu, *Electrochimica Acta*, 90 (2013) 350.
15. D. Wang, Y. Huang, Z. Huo and L. Chen, *Electrochimica Acta*, 107 (2013) 461.
16. S. H. Kang, J. Kim, M. E. Stoll, D. Abraham and K. Amine, *J. Power Sources*, 112 (2002) 41.
17. S. H. Kang, K. Amine, *J. Power Sources*, 120 (2003) 150.
18. J. Wilcox, S. B. Patoux and M. Doeff, *J. Electrochem.Soc*, 85 (2012) 411.
19. C. J. Jafta, K. I. Ozoemena, M. K. Mathe and W. D. Roos, *Electrochimica Acta*, 85 (2012) 411.
20. S. U. Woo, B. C. Park, C. S. Yoon, S. T. Myung and J. Prakash, *J. Electrochem.Soc*, 154 (2007) A649.
21. S. H. Kang, P. Kempgens, S. Greenbaum and A. J. Kropf, *J. Materials Chemistry*, 17 (2007) 2069.
22. Z. L. Gong, H. S. Liu, X. J. Guo, Z. R. Zhang and Y. Yang, *J. Power Sources*, 136 (2004) 141.
23. Liu, X, T. Huang and A. Yu, *Electrochimica Acta*, 133 (2014) 556.
24. Y. Zang, C. X. Ding, X. C. Wang, Z. Y. Wen and C. H. Chen, *Electrochimica Acta*, 168 (2015) 235.
25. J. M. Zheng, X. B. Wu and Y. Yang, *Electrochimica Acta*, 56 (2011) 3074.

26. K. A. Jarvis, Z. Deng, L. F. Allard, A. Manthiram and P. J. Ferreira, *C. Materials*, 23 (2011) 3616.
27. X. Jin, Q. Xu, X. Yuan, L. Zhou and Y. Xia, *Electrochimica Acta*, 114 (2013) 607.
28. Y. Wu, A. Manthium, *J. Power Sources*, 183 (2008) 749.
29. Y. S. Meng, G. Ceder, C. P. Grey, W. S. Yoon and S. H. Yang, *E. Solid-State Lett*, 7 (2004) 155.
30. M. M. Thackeray, S. H. Kang, C. S. Johnson and R. Benedek, *J. Mater. Chem*, 14 (2007) 3053.
31. J. Breger, M. Jiang, N. Duper, Y. S. Meng and Y. Shao, *J. Solid State Chem* 178 (2005) 2575.
32. A. Boulineau, L. Croguennec, C. Delmas and F. Weill, *S. State Ion*, 180 (2010) 35.
33. D. Wang, Y. Huang, Z. Huo and L. Chen, *Electrochimica Acta*, 107 (2013) 463.
34. S. W. Woo, S. T. Myung, H. Bang, D. W. Kim and Y. K. Sun, *Electrochimica Acta*, 54 (2009) 3852.
35. L. Li, B. H. Song, Y. L. Chang, H. Xia, J. R. Yang and K. S. Lee, *J. Power Sources*, 283 (2015) 163.